Removal of Diesel Oil from Aqueous Solution Using Agro-Waste Activated Carbon Synthesized by Chemical and Microwave Activation

Estapraq Ameen Taki[1], Sami D. Salman[1*]

[1] Biochemical Engineering Department, Al-Khwarizmi College of Engineering, University of Baghdad, Baghdad 47024, Iraq

* Corresponding author's e-mail: sami@kecbu.uobaghdad.edu.iq

ABSTRACT

In this article, buckthorn twigs were used to prepare activated carbon preparation by chemical activation with a microwave technique for removing diesel oil from water. buckthorn twigs and activated carbon were characterized by field emission scanning electron microscopy (FESEM), energy dispersive X-ray (EDX), and Fourier transform infrared (FTIR) analysis techniques. Design-Expert (13 Stat-Ease) with response surface methodology (RSM) was selected to identify and analyze the effects of activated carbon preparation factors. These factors include impregnation ratio, impregnation time, and microwave power with exposure time on the adsorption of methylene blue dye. Likewise, the effects of adsorption factors including; diesel oil concentration, pH, adsorption time, and adsorbent dosage on the removal efficiency were studied. The results showed that the maximum removal efficiency was 96.0823% with the significance of all adsorption factors. The adsorption data were fitted with the adsorption isotherm and kinetics models. The results showed that Freundlich and second-order kinetic models well described diesel oil adsorption, thus elucidating the applicability of multilayer and chemosorption processes. In addition, the thermodynamics parameters of diesel oil adsorption were determined, and the results demonstrated a spontaneous and endothermic adsorption process.

Keywords: activated carbon, adsorption, diesel oil, response surface methodology, chemical and microwave activation.

INTRODUCTION

The effluents of petroleum products into the environment via human activities threaten all life forms of microbial species, and human communities due to immunotoxic, carcinogenic, and mutagenic effects (Chikere et al. 2011). The aromatic and aliphatic petroleum products, such as toluene, benzene, diesel oil, …etc, are entered into the environment as a result of chemical and petrochemical processes like; distillation, extraction, thermal cracking, isomerization and transportation (Al-Futaisi et al. 2007; Rasouli et al. 2017). The environmental petroleum pollutants have aroused the wide attention of researchers due to their harmful effects on the ecosystem (Machín-Ramírez et al. 2008). The presence of petroleum products especially diesel fuel may form oil-water emulsions which constitute a severe hazard to the environment and aquatic health (Abdulredha et al.

2020) Therefore, different methods were applied for oily wastewater treatment such as; mechanical, biological, chemical, and physicochemical methods (Azimi et al. 2005; Abdulredha et al. 2020). Chemical methods for hydrocarbon and oil slicks treatment used dispersants as surfactants (Pan et al. 2007), or chemical oxidation by the Fenton method (Abdulredha et al. 2020). However, despite their good performance, these methods are considered energy-intensive and have high operating costs (Ewis et al. 2022). The adsorption method is considered one of the effective physical methods for removing organic pollutants, so It has drawn a lot of scientific interest in various environmental domains (Diaz de Tuesta et al. 2018). A promising alternative treatment approach that is rarely used to treat oily wastewater is activated carbon adsorption (SeyedHosseini & Fatemi 2013). In general, activated carbon in powdered or granular forms mainly has an excellent adsorption

capability for organic or non-organic contaminants due to their porosity, and specific surface area (Tseng & Tseng 2005; Erto et al. 2017; Wei et al. 2018; Salman 2020; Salman et al. 2021; Jabbar et al. 2022; Salman et al. 2023). Coal, wood, and coconut shells were widely used as raw materials for the industrial production of activated carbon (Saleem et al. 2019). However, these materials are expensive, thus it is necessary to achieve cheap and obtainable raw materials for activated carbon preparation. Different agricultural by-products were used to prepare activated carbon for wastewater treatment research including soft, low-density, and compressible raw material such as potato peel waste (Osman et al. 2019; Salman & Rashid 2024), rice bran and rice husks (Suzuki et al. 2007; Menya et al. 2018), cotton stalk (Özdemir et al. 2011), sugarcane bagasse (Guo et al. 2020), straws (Li et al. 2021), waste tea (Yagmur et al. 2008), banana peels (Ingole et al. 2017), orange peels (Fernandez et al. 2014), potato peels, tobacco stems (Li et al. 2008) corn biomass (Doczekalska et al. 2022), sawdust (K. Shakir 2010; Khalid & Salman 2019), peanut shells and soybean stover (Ahmad et al. 2012). Likewise, dense, and non-compressible by-products such as date stones (Foo & Hameed 2011), walnut shells (Nowicki et al. 2010), date palm fronds (2022) Siri's seed pods (Ahmed & Theydan 2013a, b) apricot seed (Salman et al. 2023), olive stone (Yeddou et al. 2010; Hazzaa & Hussein 2015; Saleem et al. 2019). Whereas, a few studies were implemented for aromatic and diesel oil adsorption (Yang et al. 2018; Cai et al. 2019b). Therefore, this paper presents buckthorn twigs as a low-cost precursor for activated carbon preparation by pyro carbonic acid microwave technique (Yang et al. 2017). The activated carbon is used to investigate the adsorption of diesel oil from aqueous solution. The physiochemical characteristics of precursor and activated carbon were analyzed by BET, SEM, and FTIR. Design of experiment was selected with response surface methodology (RSM) to study the effects of acid impregnation ratio, impregnation time, microwave power, and time on the methylene blue adsorption capacity as indication of activated carbon surface area. Likewise, the effects of diesel oil concentration, pH of the solution, adsorption time, and adsorbents dose on the removal efficiency were investigated. In addition, the adsorption isotherm and kinetics model as well as the thermodynamics parameters were studied to evaluate diesel oil water.

MATERIALS AND METHODS

All chemicals, gases and experimental setup used in this research are listed in Table 1.

Adsorbent preparation

The Buckthorn plant twigs were collected from the gardens of AL Khwarizmi College of Engineering / University of Baghdad. The samples were cut into pieces about 1 cm, and washed to remove dirt before being processed. The sample was dried in a dryer to the temperature of 105 ºC for overnight, then crushed and sieved to mesh size 1–2 mm. The activated carbon was prepared using the pyrocarbonic acid-microwave method (Jiang & Sun 2017). The pulverized sample was mixed with 60% phosphoric acid, which is considered a chemical activation agent, and the mixture was transferred to a glass reactor placed in a microwave oven for irradiation (activation) at a different microwave power and activation time under a nitrogen atmosphere. The activated carbon produced was cooled to room temperature,

Table 1. Chemicals, gases and experimental setup

Material	Chemical formula	Purity	Source	Usage
Buckthorn twigs	–	–	Local	Precursor
Phosphoric acid	H_3PO_4	85%	India	Chemical activating agent
Sodium hydroxide	NaOH	90%	Sigma-Aldrich Germany	Solution pH adjustment
Distilled water	H_2O	100%	Local	Washing
Nitrogen	N_2	99.9%	Local	Inert gas for microwave carbonization
Methylene blue dye	KCN	BioUltra, ≥ 98%	Sigma-Aldrich Germany	(MBN)
Diesel oil	$C_{12}H_{13}$	–	Local	Aqueous pollutant
Microwave oven (700 W)	–	–		Activated carbon preparation

washed with distilled water to remove acid residue until pH reached about 6.5–7, and then dried at 105°C for 24 hours.

Methylene blue number

Methylene blue number (MBN) is a parameter that gives the adsorption capacity of activated carbon using methylene blue dye. This could be used due to its simplicity and rapid assessment of adsorbent quality. a stock solution of methylene blue dye concentration 50 mg/L was prepared by dissolving 50 mg of methylene blue in 1000 cm^3 of distilled water. Set of ten measuring flasks with 10 cm^3 using volume batch of 0.025; 0.05; 0.1; 0.2; 0.4; 0.5; 0.8; 1.0; 2.0; and 4 cm^3 of stock solution and diluted to 10 cm^3 using distilled water to obtained 0.125; 0.25; 0.5; 1; 2; 2.5; 4; 5; 10; and 20 mg/L. The intermediate concentrations as a blank solution and after adsorption using 1 g of activated carbon were measured using UV– visible spectroscopy ($\lambda = 660$ nm). The adsorption capacity of methylene blue dye using 1 g of activated carbon produced was determined using equation 1.

$$MBN = \frac{(c_o - c_e)V}{W} \tag{1}$$

where: C_o and C_e are methylene blue dye's initial concentration and final concentration at equilibrium (mg/L), *MBN* is the adsorption capacity in g of dye per g of activated carbon (g/g), *V* is the volume dye solution (mL), and *W* is the mass of activated carbon (g).

Adsorbate experiments

To evaluate the removal efficiency of diesel oil adsorption by activated carbon, diesel oil supplied from midland refineries company to prepare 1000 mg/L of diesel oil solution by mixing about 1 g of diesel oil with 1000 mL of distilled water. The diesel oil concentration range 100–500 mg/L was prepared by dilution with distilled water in a series of Erlenmeyer flasks. The flasks were fixed on a thermostatic oscillator for 30 min and 150 rpm to produce an oily water solution. The effects of initial concentration (100–500 mg/L), adsorbent dosage (0.1–0.5 g), contact time (10–360 min), and pH on the adsorption capacity and removal efficiency were investigated. The pH of the diesel oil solution was adjusted to 4.0, 6.0,

7.0, 8.0, and 10.0 by 1 M HCl or 0.1 M NaOH. The diesel oil concentration before and after adsorption was measured using a UV-vis spectrophotometer (UV-1800, SHIMADZU, Japan) at a wavelength of 256 nm. The adsorption capacity and removal efficiency were calculated using equations 2, and 3.

$$q_e = \frac{(c_o - c_e)}{W} \times V \tag{2}$$

$$RE\% = \frac{(c_o - c_e)}{c_o} \times 100\% \tag{3}$$

where: C_o and C_e are the initial and final concentration of diesel oil (mg/L), *V* is the volume dye solution (L), *W* is the mass of activated carbon (g), q_e is the adsorption capacity (mg/g), and *RE* is the removal efficiency.

Design experiment for activated carbon preparation

Small pieces of Buckthorn twigs were collected from the gardens of Al-Khwarizmi College of Engineering. The twigs were washed with distilled water to remove dust and dirt, then dried overnight in an air dryer at 105 ºC. The dried twigs were crushed and sieved to 1–2 mm, then the samples were impregnated in 60% of H$_3$PO$_4$ with impregnated ratio 1–3, with impregnation time 3–9 h. The impregnated samples were poured into a glass reactor and transferred to multi-power microwave oven for activation. Different power 420–700 W with different time intervals 8–24 min were selected under nitrogen atmosphere for activation to produce activated carbon. The activated carbon transferred to Buchner funnel filter and cleaned with hot water to remove any remaining acid residue until pH reached 6.5–7, then the samples were dried in an air dryer at 105°C for 24 hr and the dried samples were crushed to the desired particle size (Salman & Rashid). Design Expert Software (13 Stat-Ease) was selected with Box-Behnken design (BBD) methodology to study the factors effect of impregnation ratio, time of impregnation, microwave power, and time of activation as independent factors on methylene blue dye capacity MBN as shown in Table 2. A number of experiments were generated by the software as shown in Table 3.

It's noted from Table 3, that MBN was obtained from run number 9. Therefore, this sample was selected for further characterization and adsorption of diesel oil from an aqueous solution.

Table 2. Experimental independent variables for active carbon preparation

Factor	Name	Units	Low	High
A	IR	Ratio	1:1	1:3
B	Impregnation time	hr	3	0
C	Radiation power	watt	420	700
D	Radiation time	min	8	24

Table 3. Experimental design of activated carbon preparation

Number	Impregnation ratio	Impregnation time (h)	Microwave power (W)	Activation time (min)	MBN
1	3	6	560	8	22.5002
2	3	3	560	16	24.7733
3	2	6	560	16	24.7928
4	3	6	560	24	25.1862
5	3	6	420	16	25.1261
6	1	3	560	16	25.0512
7	2	9	560	8	24.446
8	2	9	560	24	25.1045
9	2	9	420	16	25.878
10	1	6	420	16	25.1666
11	2	9	700	16	24.971
12	1	6	560	24	23.5002
13	2	3	420	16	25.0391
14	3	9	560	16	24.9082
15	1	9	560	16	25.1929
16	1	6	560	8	24.7632
17	2	6	700	24	25.1936
18	2	6	420	8	25.0492
19	2	3	700	16	25.1977
20	2	6	700	8	23.195
21	3	6	700	16	23.5002
22	2	6	420	24	24.9426
23	2	3	560	24	25.1977
24	1	6	700	16	25.0236
25	2	3	560	8	23.8975
26	2	6	560	18	25.1929

RESULTS AND DISCUSSION

Characterization

Brunauer-Emmett-Teller analysis

Brunaure-Emmett-Teller (BET) HORIBA, SA-900 series, USA, using the liquid nitrogen adsorption-desorption isotherm to determine the specific surface area with pore size of buckthorn and activated carbon sample (run number 9) as shown in Table 4. It's noted from this table that the BET surface areas of the buckthorn twigs powder have 2.76 m^2/g with pore size 7.07 nm, and the surface area of activated carbon produced was 1305.15 m^2/g with pore size 2.7 nm. Similar results were obtained for activated carbon prepared from Ficus Benjamin using the microwave technique (Talib & Salman 2023).

FESEM analysis

The surface morphology for the buckthorn plant, activated carbon, and its composite are

Table 4. Specific surface area with pore size for raw material and AC

Sample	Test name	Results	Method	Detection limit	Uncertainty value
BP	Surface area (m^2/g)	2.76	ISO 9277/2010	0.0005 m^2/g	0.182%
	Pore size (nm)	7.07			
AC	Surface area (m^2/g)	1305.15			
	Pore size (nm)	2.7			

shown in Figures 1 and 2. FESEM scan images of buckthorn plant as precursor material are shown in Figure 1. The buckthorn plant clarified a smooth and homogeneous surface with a very slight number of pores, whereas the surface morphology of activated carbon as shown in Figure 2 evolved into a spongy nature with different pores sizes and shapes. This may be due to the decomposition and volatilization of non-carbonaceous material in feedstock during activation and carbonization stages that caused different pore sizes and shapes (Şentorun-Shalaby et al. 2006).

In general, the formation of the pores on the surface of activated carbon increases the
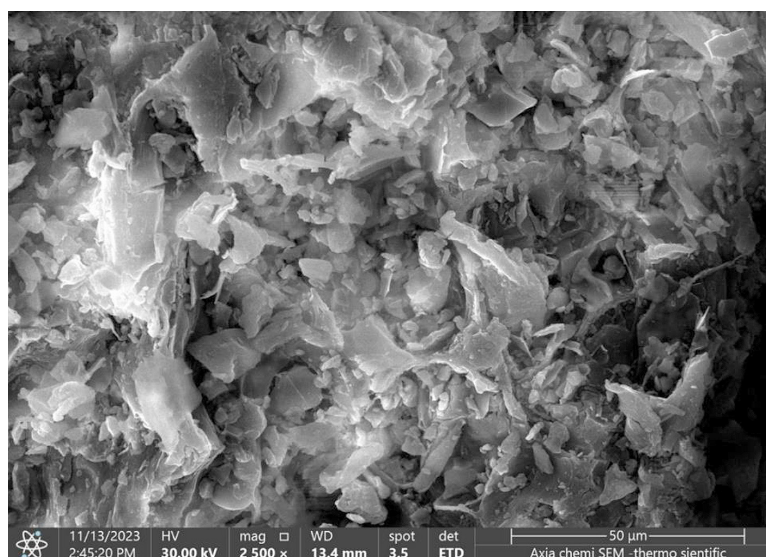
**Fig. 1.** FESEM images of buckthorn twigs powder
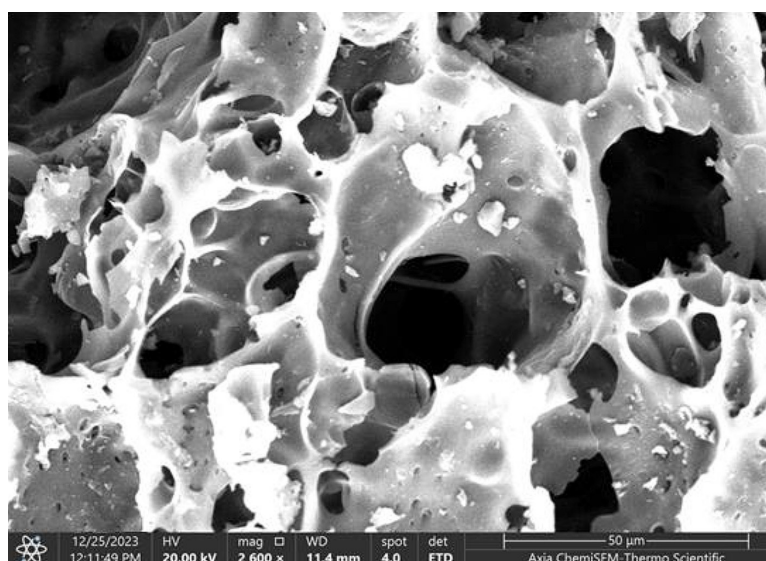

Fig. 2. FESEM images of activated carbon

possibility of diesel oil adsorption due to the diffusion and reaction of H_3PO_4 with cellulose to produce phosphate ester which decomposed simultaneously to form micropore due to the activation and carbonization. The elemental compositions of raw materials and activated carbon were investigated using spectroscopic EDX techniques, and their results shown in Figures 3, 4 and Tables 5 and 6. The data reveal that the activation and carbonization increased the carbon contents from 36.1% for buckthorn plant to 86.4% for activated carbon produced. Whereas, the elemental contents were changed due to the increases of activated carbon during the activation and carbonization stages (Salman et al. 2023).

FTIR analysis

The FTIR spectra for buckthorn plant (BP), and activated carbon (BPAC) at wavelength range 4000 and 400 cm^{-1} are deprecated in Figure 5. The raw material appears several peaks reflect the complex nature of the buckthorn powder. The peaks between 3500–4000 cm^{-1} were caused by the OH stretching vibration, due to the presence of alcohols, chemisorbed water, and phenols (Nasrullah et al. 2015). The absorption peaks between 2500–3500 cm^{-1} are caused by -CH, $-CH_2$, and other saturated aliphatic groups. Likewise, the peak at 2300 cm^{-1} is due OH band and the peaks between 1500–2000 cm^{-1}
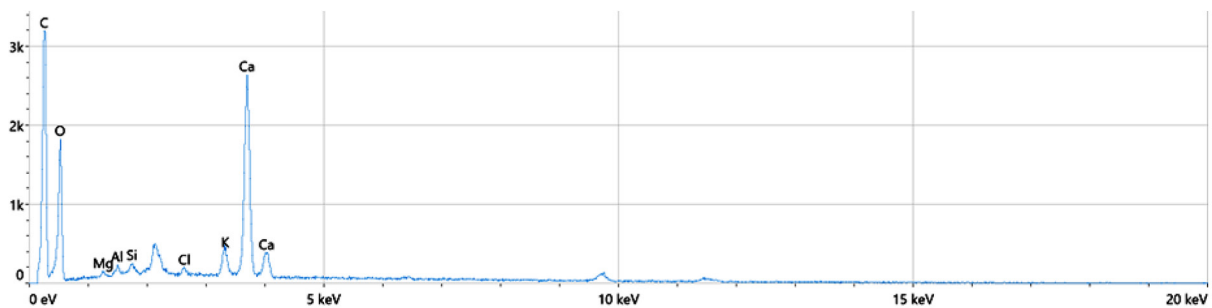
**Fig. 3.** Energy dispersive X-ray (EDX) spectroscopy of raw material
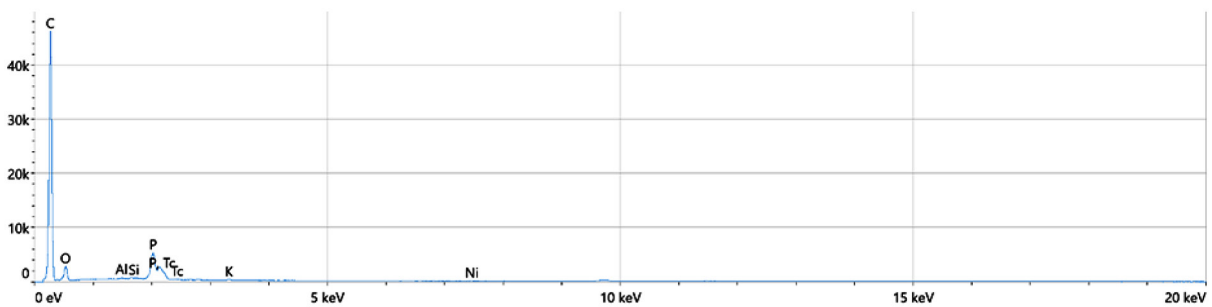
Fig. 4. Energy dispersive X-ray (EDX) spectroscopy of activated carbon

Table 5. Elemental composition of raw material

Element	Atomic %	Atomic % error	Weight %	Weight % error
C	46.7	1.0	36.1	0.7
O	47	1.0	48.4	1.0
Mg	0.2	0.1	0.3	0.1
Al	0.3	0.1	0.5	0.1
Si	0.3	0.0	0.6	0.1
Cl	0.2	0.0	0.4	0.1
K	0.6	0.1	1.5	0.5
Ca	4.7	0.2	12.2	0.9

Table 6. Elemental composition of elemental composition of activated carbon

Element	Atomic %	Atomic % error	Weight %	Weight % error
C	83.3	0.4	86.4	0.3
O	14.5	0.2	7.7	0.2
Al	0.0	0.0	0.0	0.0
Si	0.1	0.0	0.2	0.0
P	1.8	0.0	4.2	0.1
K	0.1	0.0	0.2	0.0
Ni	0.1	0.0	0.3	0.1
Tc	0.1	0.0	1.0	0.1
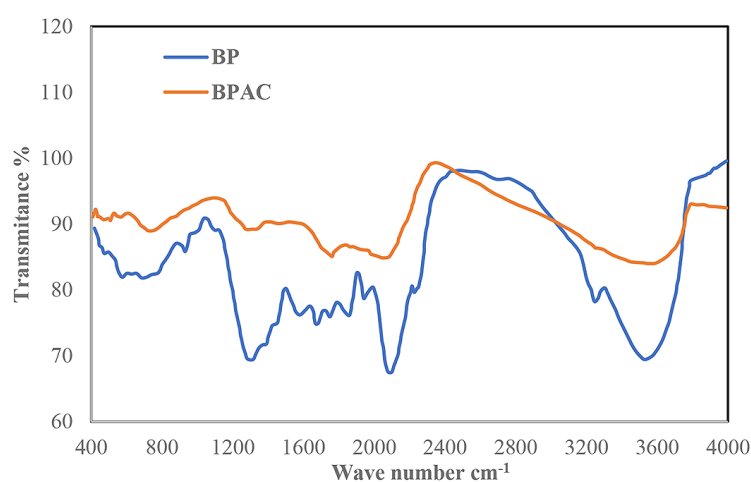
Fig. 5. FTIR spectra of Buckthorn plant (BP), and activated carbon (BPAC)

refer to the presence of COOH. The peaks between 1000–1500 cm^{-1} indicate aldehyde C=O and phenol C=C groups and the peaks between 500–1000 cm^{-1} refer to the vibrational bending of the aromatic compounds (Khare & Baruah 2010; Taşar et al. 2014). In addition, many peaks disappeared due to activation and the others appear due to new bond formation in activated carbon. Therefore the peaks observed between 3500–4000 cm^{-1} are ascribed to the oscillation of the stretching bond of free hydrogen bound to −OH groups (Nasrullah et al. 2015). The absorption bands between 2500–3000 cm^{-1} are related to the C-O stretching vibration bond of carbon dioxide or carbon monoxide. The peak between 2000–2500 cm^{-1} corresponds to bond stretching vibrations of alkynes (C≡C) and the peaks between 1500–2000 cm^{-1} are related to the stretching vibration of C=C (Benzaoui et al. 2018). Whereas the peaks between 1000–1500 cm^{-1} are assigned to symmetric and antisymmetric stretching of (N=O) and C-O-C (Labied et al. 2018). Furthermore, the peaks around 1100–1200 cm^{-1} could be attributed to stretching mode of hydrogen-bonded P=O, to O–C stretching vibrations in P–O–C (aromatic) linkage and to P= OOH (Puziy et al. 2002), and the peaks around 800 cm^{-1} could be assigned to out-of-plane bending vibrations of C-H group in the aromatic rings (Allwar 2012).

Experimental design for diesel oil adsorption

Batch experiments were carried out with 200 ml as a working volume at room temperature and constant speed of agitation (200 rpm). Design-Expert software (version 13 Stat-Ease) using RSM with I-Optimal technique was applied to evaluate the effect of contact time, initial pH, diesel oil concentration, the dosage of adsorbent, and their interaction on the removal efficiency. Five levels were selected to explore the entire range of adsorption conditions and to identify the optimum operating variables. The experimental runs using I-Optimal technique was generated as shown in Table 7, and 8.

Table 7. Independent factors for diesel oil adsorption (December 21, 2020)

Factor	Name	Unit	Levels				
A	Diesel oil concentration	mg/L	100	200	300	400	500
B	pH	pH	4	6	7	8	10
C	Contact time	min	15	60	180	240	360
D	Dose of AC	g/200mL	0.1	0.2	0.3	0.4	0.5

Table 8. Experimental runs using RSM with I-Optimal method (December 21, 2020)

Run	Factor 1 A: conc mg/L	Factor 2 B: pH pH	Factor 3 C: time min	Factor 4 D: dosage g/200ml	Response 1 RE1 %
1	500	8	180	0.4	93.6028
2	200	8	360	0.5	88.2095
3	100	6	360	0.1	69.201
4	300	7	15	0.3	94.404
5	500	4	360	0.1	88.2588
6	100	10	60	0.4	53.455
7	400	6	180	0.1	96.0823
8	100	4	360	0.5	83.597
9	200	4	240	0.3	88.926
10	100	4	15	0.1	63.746
11	400	6	180	0.1	96.0823
12	500	4	15	0.2	92.4016
13	300	7	180	0.5	94.465
14	200	4	240	0.3	88.926
15	100	6	15	0.5	62.581
16	500	4	360	0.4	91.8776
17	400	10	360	0.2	83.3955
18	500	10	15	0.1	86.2022
19	100	7	240	0.3	69.763
20	100	10	180	0.2	54.676
21	300	10	15	0.5	79.146
22	300	7	15	0.3	94.404
23	500	8	180	0.4	93.6276
24	300	7	15	0.3	94.404
25	400	4	60	0.5	83.2163

Statistical data analysis of diesel oil removal efficiency

The statistical analysis (ANOVA) of the quadratic models for diesel oil removal efficiencies by activated carbon (Y) using I-Optimal method is illustrated in Table 9 It's concluded from the tables that the model coefficients with their interaction are indicated as significant depending on the p-value ($p<0.05$). The quadric model for Y which was selected for analysis and optimization is shown in Equations 4, and Table 10.

$$Y = a_o + a_1 A + a_2 B + a_3 C + a_4 D + a_{12} AB + a_{13} AC + a_{14} AD + a_{23} BC + a_{24} BD + a_{34} CD + a_{11} A^2 + a_{22} B^2 + a_{33} C^2 X_3^2 + a_{44} D^2 \tag{4}$$

where: Y is the removal efficiency of diesel oil by activated carbon, a_0 is intercept a_1, a_2, a_3, and a_4 are linear coefficients, a_{12}, a_{13}, a_{14}, a_{23}, and a_{34} are second-order interaction terms, and a_{11}, a_{22}, a_{33}, and a_{44}, are quadratic terms for each factor. A, B, C, and D, are diesel oil concentration, pH

Table 9. ANOVA for removal efficiency (Y_1) quadratic model

Source	Sum of squares	df	Mean square	F-value	p-value	
Model	4199.08	14	299.93	91.49	<0.0001	significant
A-conc	1892.85	1	1892.85	577.40	<0.0001	
B-pH	351.06	1	351.06	107.09	<0.0001	
C-time	75.05	1	75.05	22.89	0.0007	
D-dosage	16.31	1	16.31	4.97	0.0498	
AB	68.77	1	68.77	20.98	0.0010	
AC	56.99	1	56.99	17.38	0.0019	
AD	28.57	1	28.57	8.71	0.0145	
BC	40.81	1	40.81	12.45	0.0055	
BD	22.53	1	22.53	6.87	0.0255	
CD	104.05	1	104.05	31.74	0.0002	
A²	628.27	1	628.27	191.65	<0.0001	
B²	199.52	1	199.52	60.86	<0.0001	
C²	0.0148	1	0.0148	0.0045	0.9477	
D²	70.68	1	70.68	21.56	0.0009	
Residual	32.78	10	3.28			
Lack of fit	32.78	5	6.56	1.066E+05	<0.0001	significant
Pure error	0.0003	5	0.0001			
Cor total	4231.87	24				

Table 10. Removal efficiency coefficients

Coefficient symbol	Coefficient value
a_0	20.18064
a_1	0.246848
a_2	7.00536
a_3	0.038185
a_4	40.84898
a_{12}	0.00518
a_{13}	-0.000081
a_{14}	-0.051742
a_{23}	-0.004532
a_{24}	3.34291
a_{11}	0.108854
a_{22}	-0.00032
a_{33}	-0.751684
a_{44}	-1.93E-06
a_0	-105.13709

of solution, contact time, and adsorbent dose, respectively.

The removal efficiency models offered reasonable agreement between the predicted R^2 = 0.79248, and adjusted R^2 = 0.9143; i.e. the deference less than 0.2 (December 21, 2020). In order to check the accuracy and validity of these models, the error percentage between the experimental data and models predicted data were calculated as shown in Table 11. It's noted from this table that the average percentage error was found to be 1.074575% (<5%) which mean that the predicted value has more than 95% accuracy and validate.

Surface response analysis of diesel oil removal efficiency

Three and two-dimensional plots were used to visualize the response surface plots and contour plots of the main independent variables (factors) with their significant interaction effects on the removal efficiency of diesel oil by activated carbon. Therefore, the effects oil concentration (100–500 mg/L), contact time (15–360 min), pH (4–10), and adsorbent dose (0.1–0.5 g) on removal efficiency is visualized for optimization depending on their p-values (p<0.05) as mentioned before in Table 8.

Effect of initial concentration and contact time on the removal efficiency

In this section, the effects of diesel oil concentration with contact time on the removal efficiency at constant pH and adsorbent dose of activated carbon are discussed based on surface

Table 11. Validation of predicted diesel oil removal efficiency model with experimental results

Run	Factor 1 A: conc mg/L	Factor 2 B: pH pH	Factor 3 C: time min	Factor 4 D: dosage g/200ml	Actual RE %	Predicted RE %	Percentage error %
1	500	8	180	0.4	93.6028	92.96	0.686732
2	200	8	360	0.5	88.2095	89.52	1.485668
3	100	6	360	0.1	69.201	68.98	0.31936
4	300	7	15	0.3	94.404	93.90	0.533876
5	500	4	360	0.1	88.2588	88.05	0.236577
6	100	10	60	0.4	53.455	54.24	1.468525
7	400	6	180	0.1	96.0823	96.14	0.060053
8	100	4	360	0.5	83.597	81.62	2.364917
9	200	4	240	0.3	88.926	89.24	0.353103
10	100	4	15	0.1	63.746	63.93	0.288646
11	400	6	180	0.1	96.0823	96.14	0.060053
12	500	4	15	0.2	92.4016	91.44	1.040675
13	300	7	180	0.5	94.465	93.12	1.423808
14	200	4	240	0.3	88.926	89.24	0.353103
15	100	6	15	0.5	62.581	62.19	0.62479
16	500	4	360	0.4	91.8776	92.54	0.720959
17	400	10	360	0.2	83.3955	83.19	0.246416
18	500	10	15	0.1	86.2022	87.63	1.656338
19	100	7	240	0.3	69.763	73.09	4.769004
20	100	10	180	0.2	54.676	52.46	4.052967
21	300	10	15	0.5	79.146	79.30	0.194577
22	300	7	15	0.3	94.404	93.90	0.533876
23	500	8	180	0.4	93.6276	92.96	0.713038
24	300	7	15	0.3	94.404	93.90	0.533876
25	400	4	60	0.5	83.2163	85.00	2.14345
Average error %							1.074575

response analysis as illustrated in Figures 6, and 7, respectively. It's clearly noted that the removal efficiencies for activated carbon and composite activated carbon have similar trends. Furthermore, the removal efficiencies for two adsorbents were increased with the increases of diesel oil concentration with contact or mixing time. The maximum removal efficiencies occurred at 400 mg/L with contact time 180 min, the removal efficiencies were decreased with diesel oil concentration and time. It's clear that the rate of diesel oil adsorption rapidly increased with time in the beginning due to the availability of a large number of active sites on the surfaces of the adsorbents. After that, as the concentration increased with time, the rate of the adsorption was attenuated due to the limitation of unoccupied sites and increasing of the repulsion forces between the adsorbate molecules near the surfaces of the adsorbents and bulk solution

(Salman et al. 2011; Djilani et al. 2012; Salman & Rashid 2024).

Effect of initial concentration and pH on the removal efficiency

The variation in pH of the solution announced its acidic and alkaline environment which affected on the oil emulsion stability and functional groups in the adsorbent adsorption sites (Farah et al. 2007; Gmach et al. 2019). Therefore, the effect of diesel oil concentration with the pH of the solution on the removal efficiency using activated carbon is studied and illustrated in Figures 8, and 9. It's noted that the removal efficiency increased with increasing of diesel oil initial concentration with the pH of the solution and it reach to maximum removal efficiency at a certain point of the concentration and pH (400 mg/L and pH 6), then the removal efficiency decreased
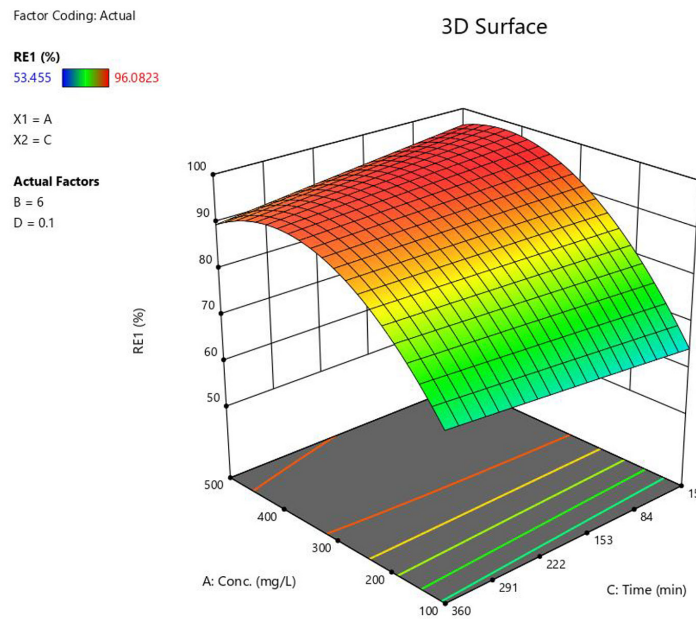
Fig. 6. 3D plot of initial concentration and contact time effects on removal efficiency using AC
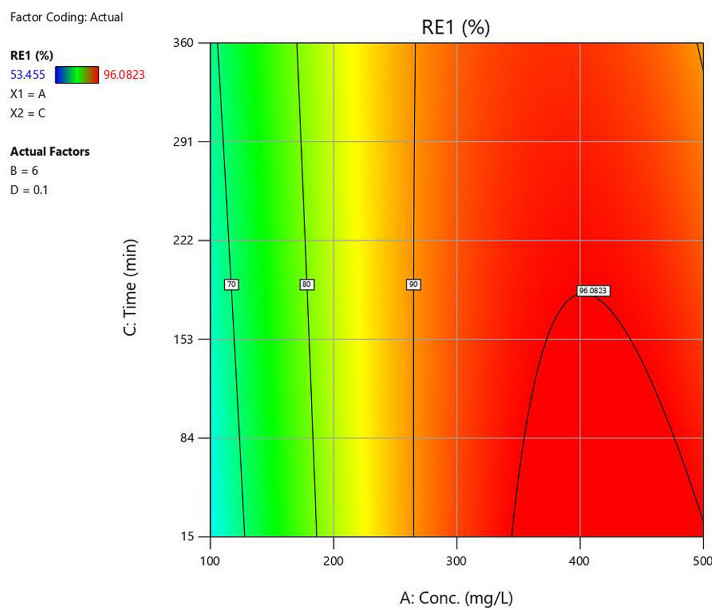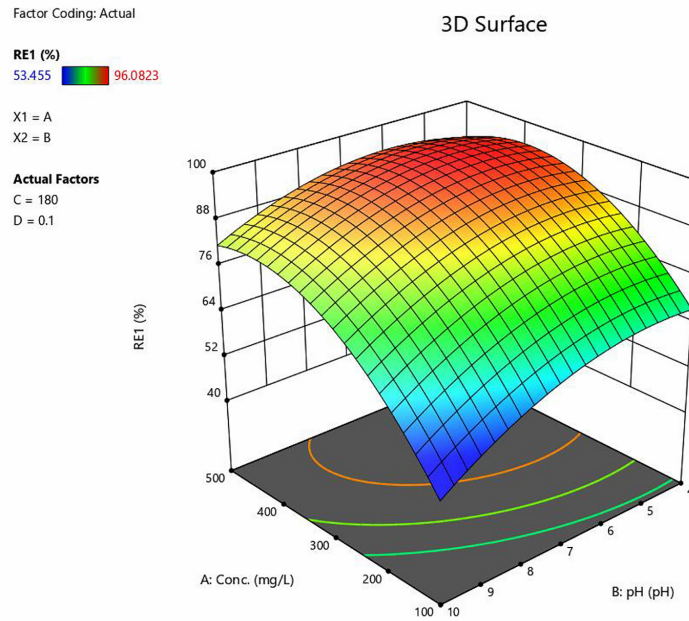

Fig. 7. 2D plot of initial concentration and contact time effects on removal efficiency using AC

with increasing of diesel oil initial concentration with the pH of the solution. These implied that the more acidic and alkaline environments are not suitable for diesel oil adsorption into the adsorbent surface. This means that large number of protons were accessible at lower pH levels, which saturated the adsorbent sites and increased the adsorbent surface cationic characteristics (Ahmad et al. 2005). As the pH of the solution increased to more than 7, an overabundance of hydroxyl ions competed with the pollutant on

the adsorption active sites, resulting in decreased diesel oil sorption (Zhang et al. 2017).

Effect of initial concentration and adsorbent dose on the removal efficiency

The effect of diesel oil concentration with an adsorbent dose on removal efficiency using activated carbon is clarified in Figures 10 and 11. It's noted from these figures that the removal efficiency increases mainly depend on the increase of

Fig. 8. 3D plot of initial concentration and pH effects on removal efficiency using AC
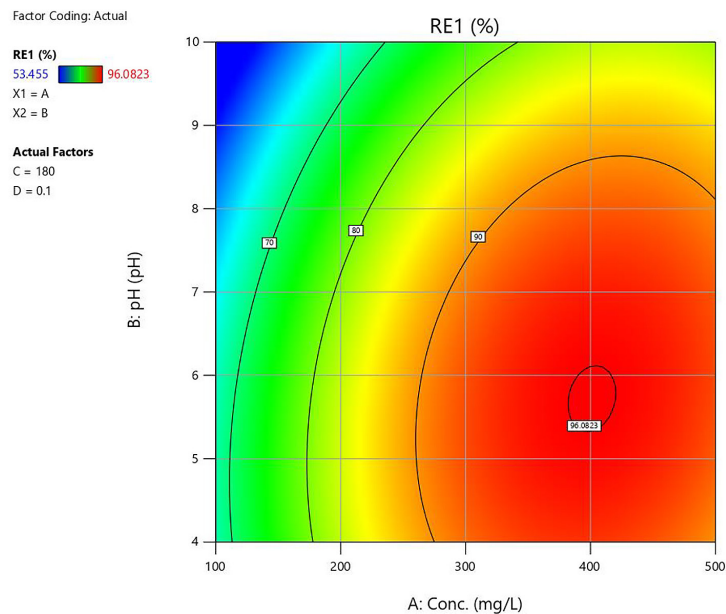
Fig. 9. 2D plot of initial concentration and pH effects on removal efficiency using AC

diesel oil initial concentration as compared to the adsorbent dose. This means that minimum adsorbent dose was sufficient for all diesel concentrations. Therefore, the maximum removal efficiency was obtained at 400 mg/L of diesel oil with minimum dose concentration (0.1 mg/200 mL), then as long as diesel oil increased the removal efficiency slightly decreased with increasing diesel oil concentration for all adsorbent doses. This may be explained by the fact that the surface area of adsorbents at minimum dose offered a large number of active sites for adsorption (Vaghetti et al. 2009). Then, as the oil concentration increased more than 400 mg/L, the rate of the adsorption was attenuated due to the limitation of unoccupied sites and increasing of the repulsion forces between the adsorbates molecules near the surfaces of the adsorbents and bulk solution (Salman et al. 2011; Djilani et al. 2012; Salman & Rashid 2024). Furthermore, as the adsorbent dose increased the removal efficiency decreased, this may be caused by an aggregation of higher
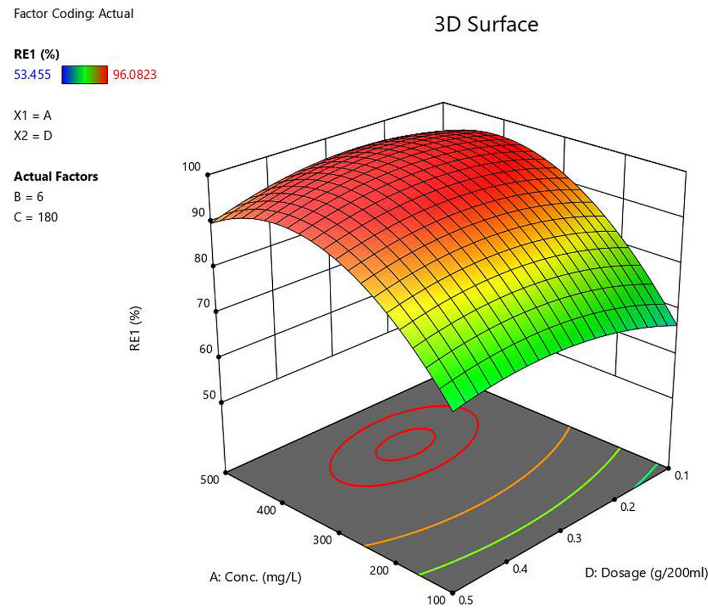
Fig. 10. 3D plot of initial concentration and dose effects on removal efficiency using AC
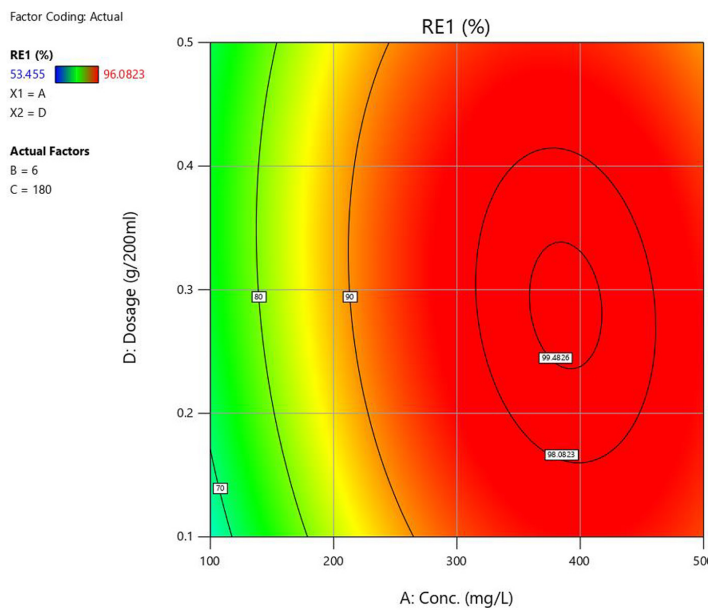

Fig. 11. 2D plot of initial concentration and dose effects on removal efficiency using AC

adsorbent doses which decreased its surface area. In addition, it may be caused by inadequate pollutant ions as compared to the available binding sites or by the interference between the higher adsorbent dose and binding sites (El Shahawy & Heikal 2018; Mohammed et al. 2020).

Adsorption isotherm studies

In order to identify the behavior of adsorbate molecules at a solid-liquid phase as mono or multilayer adsorption, the adsorption experimental data for different adsorbents are fitted with the most widespread adsorption isotherm models Langmuir (Langmuir 1917) and Freundlich (Van der Bruggen 2015) were used for diesel oil adsorption data assessment using different adsorbents. The linear forms of the Langmuir and Freundlich models are illustrated in equations 5 and 6.

$$\frac{1}{q_e} = \frac{1}{q_m} + \frac{1}{k_L q_m C_e} \qquad (5)$$

$$log q_e = log k_f + \left(\frac{1}{n}\right) log C_e \qquad (6)$$

where: q_e (mg/g) is the equilibrium adsorption capacity, C_e (mg/L) is the equilibrium diesel oil concentration, k_1 (l/mg) is the adsorption equilibrium constant, q_m (mg/g) is the complete monolayer adsorption capacity, k_f (l/mg) and 1/n are Freundlich constants.

Langmuir and Freundlich isotherm models were used to describe the adsorption behavior of diesel oil on AC adsorbent illustrated in Figures 12 and 13. It noted that the adsorption process data were well fitted with the Freundlich model for AC with $R^2 = 0.9626$, as compared to the Langmuir model ($R^2 = 0.9538$), which indicates that the adsorption occurred under the premise of multilayer adsorption on the heterogeneous surface of AC. These results are consistent with the findings reported by (Cai et al. 2019a). In addition, Langmuir and Freundlich models' coefficients are summarized in Table 12.

Adsorption kinetics

Batch adsorption of diesel oil on AC adsorbent was carried out to study adsorption kinetics under ideal circumstances and with varying contact periods. When the initial concentrations were altered, the empirical model produced different outcomes. The kinetics of adsorption process describes the interactions between adsorbate and adsorbent and were studied due to their potential relevance in water pollution control. Adsorption is a process that involves the accumulation of molecules in higher concentrations called adsorbent on the surface of the adsorbate by physical or chemical forces. The physical adsorption occurred due to weak Van der Waals forces between adsorbate and adsorbent. Whereas the chemical adsorption occurred due to strong chemical forces between adsorbate and adsorbent. Adsorption kinetics can evaluate two important features of adsorption unit design: response rate and mechanism (Boehm, 2002). Two kinetic models: pseudo-first order (Lagergren 1906) and pseudo second order (Boehm, 2002) were used for adsorption data fitting as shown in equations 7, and 8.

$$ln(q_e - q_t) = lnq_e - k_1t \qquad (7)$$

$$\frac{1}{q_t} = \frac{1}{k_2 q_e^2} + \frac{t}{q_e} \qquad (8)$$

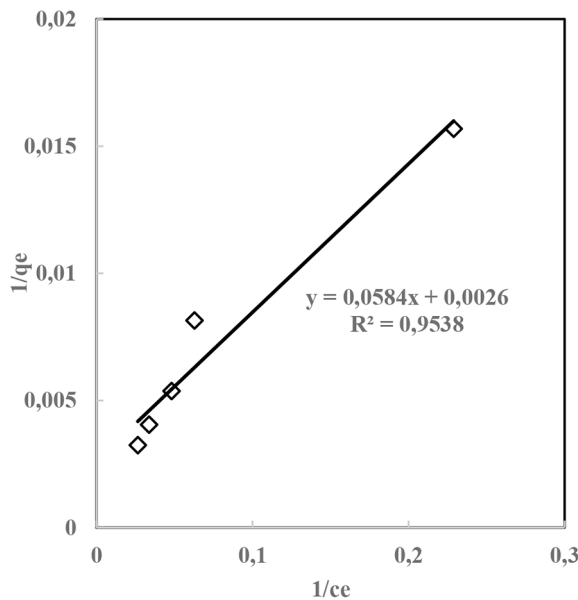where: q_e and q_t (mg/g) are the equilibrium adsorption capacities at time t (min.), k_1 (1/

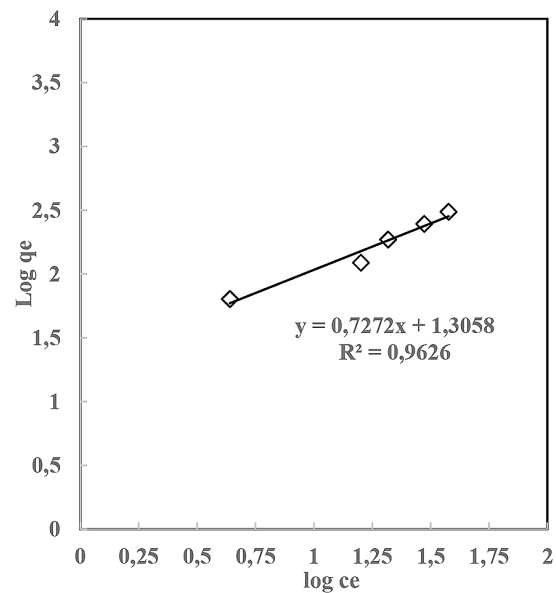**Fig. 12.** Langmuir isotherm model for diesel oil on AC adsorbent

Fig. 13. Freundlich isotherm model for diesel oil adsorption on AC adsorbent

Table 12. Freundlich and Langmuir coefficients of diesel oil adsorption on AC adsorbent

Adsorbent	Langmuir			Freundlich		
Parameter	K_L (L/mg)	q_m (mg/g)	R^2	K_f (mg/g)	n	R^2
AC	0.045	380.068	0.9538	3.9604	1.4518	0.9626

min) and k_2 (g/mg·min) are first and second-order adsorption constants.

Pseudo-first and second-order kinetic models were used to describe the mechanism of diesel oil adsorption by AC, adsorbent as illustrated in Figures 14 and 15. It noted from these figures that the adsorption process data were well fitted with the pseudo-second-order kinetic models with $R^2 = 0.9995$ as compared to the pseudo-first order kinetic model. This denoted that the diesel oil adsorption conformed with chemisorption process (Sokker et al. 2011) In addition, the pseudo-first and second-order kinetic models' coefficients for MG adsorption are summarized in Table 13.

Adsorption thermodynamic

In order to investigate the adsorption process thermodynamically the thermodynamic parameters including Gibbs free energy (ΔG), heat of enthalpy (ΔH), and entropy (ΔS) which govern the feasibility and spontaneity of the adsorption process have been calculated using equations 9, 10, and 11.

$$K_d = \frac{q_e}{c_e} \quad (9)$$

$$\Delta G = -RTlnK_d \quad (10)$$

$$\Delta G = \Delta H - T\Delta S \quad (11)$$

where: K_d (L/g) is solute coefficient distribution, C_e (mg/L) is equilibrium malachite concentration, q_e (mg/g) is equilibrium adsorption capacity, ΔG (kJ/mol) is Gibbs free energy, ΔH (kJ/mol) is heat of enthalpy, ΔS (kJ/mol·K) is entropy, and T is adsorption temperature, K.

The values of ΔG, ΔH, ΔS, and K_d were calculated based on adsorption capacity at different temperatures (25–55) °C from thermodynamic equations in Figure 16, and the values of ΔG, ΔH, and ΔS are summarized in Table 11. It's clearly noted that the values of ΔG have negative sign which implies that the adsorption process is thermodynamically feasible, favorable, and spontaneous at all temperatures. In general, the adsorption process is normally considered chemisorption when ΔH has a positive sign with a range of 20.9 to 418 kJ/mol, and physisorption with range of 2.1 to 20.9 kJ/mol (Húmpola et al. 2013). Therefore, the adsorption
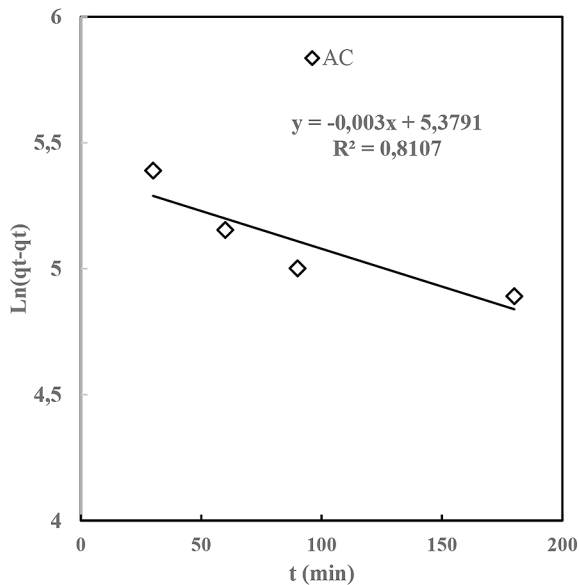
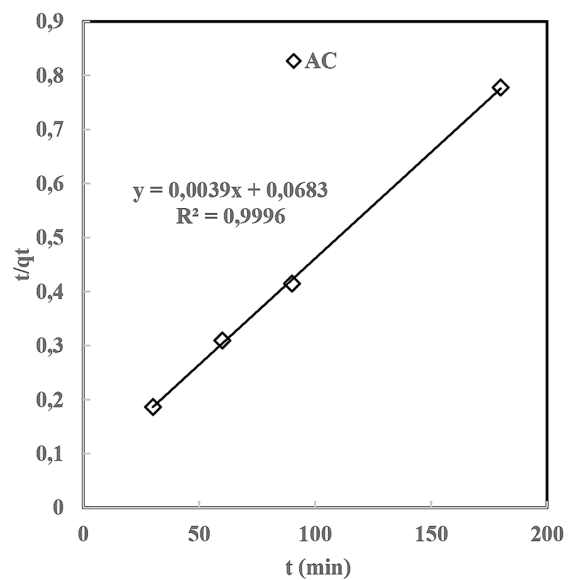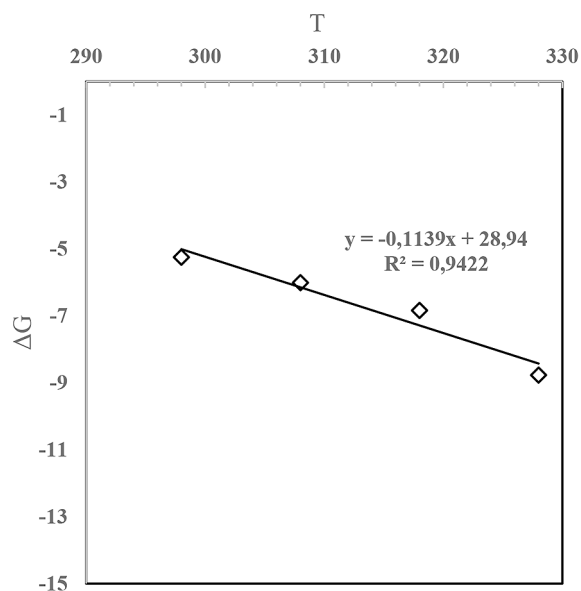**Fig. 14.** Pseudo-first-order model adsorption of diesel oil

Fig. 15. Pseudo-second-order model for adsorption of diesel oil

Table 13. The pseudo kinetic model coefficients

Adsorbent	Pseudo-first order			Pseudo-second order		
Parameter	K_1 1/min	q_e, cal mg/g	R^2	K_2 g/mg min	q_e, cal mg/g	R^2
AC	0.003	216.8233	0.8107	0.00022	254.4168	0.9995

Table 14. Thermodynamics parameters for diesel oil green adsorption

Adsorbent	Temperature (°C)	$\Delta G°$ (kJ/mol)	$\Delta H°$ (kJ/mol)	$\Delta S°$ (J/mol·K)
AC	25	-5.24946	28.9401	0.1139
	35	-6.0078		
	45	-6.8373		
	55	-8.7699		

Fig. 16. Adsorption thermodynamics for AC adsorbents

variance showed a minimum percentage error between the quadric model and observation results. In addition, the adsorption of diesel oil by activated carbon conformed with Freundlich isotherm and pseudo-second-order kinetic models which elucidated the applicability of multilayer and chemosorption process. Thermodynamic parameters obtained confirmed that the adsorption process was spontaneous, feasible, and endothermic.

Acknowledgments

process is suggested as chemisorption due to the value of ΔH obtained as shown in Table 14. In addition, the positive ΔS value implied to inconsistent increase in randomness of the diesel oil droplets arrangement at the adsorbent-solution interface during adsorption (Húmpola et al. 2013).

CONCLUSION

This study revealed that buckthorn agro-waste can be effectually used for activated carbon preparation by chemical activation and microwave technique for diesel oil removal from an aqueous solution. Design-Expert software (version 13 Stat-Ease) with Box-Behnken and I-Optimal approaches was used for analyzing the experimental data of activated carbon preparation, and diesel oil adsorption. The data analysis indicated that maximum removal efficiency was obtained with an initial concentration of diesel oil equal to 400 mg/L, contact time of 180 min, activated carbon dose of 0.1 g, and pH of solution equal to 6. The analysis of

REFERENCES

1. DESIGN EXPERT 13. 2020. Stat-Ease Inc, pp. Design Expert is a piece of software designed to help with the design and interpretation of multi-factor experiments.
2. Abdulredha, M.M., Siti Aslina, H., Luqman, C.A. 2020. Overview on petroleum emulsions, formation, influence and demulsification treatment techniques. Arabian Journal of Chemistry, 13, 3403–3428.
3. Ahmad, A.L., Bhatia, S., Ibrahim, N., Sethupathi, S. 2005. Adsorption of residual oil from palm oil mill effluent using rubber powder. Brazilian Journal of Chemical Engineering, 22.
4. Ahmad, M., Lee, S.S., Dou, X., Mohan, D., Sung, J.K., Yang, J.E., Ok, Y.S. 2012. Effects of pyrolysis temperature on soybean stover-and peanut shell-derived biochar properties and TCE adsorption in water. Bioresource Technology, 118, 536–544.
5. Ahmed, M.J., Theydan, S.K. 2013a. Microporous activated carbon from Siris seed pods by microwave-induced KOH activation for metronidazole adsorption. Journal of Analytical and Applied Pyrolysis, 99, 101–109.
6. Ahmed, M.J., Theydan, S.K. 2013b. Microwave assisted preparation of microporous activated carbon from Siris seed pods for adsorption of metronidazole

antibiotic. Chemical Engineering Journal, 214, 310–318.

7. Al-Futaisi, A., Jamrah, A., Yaghi, B., Taha, R. 2007. Assessment of alternative management techniques of tank bottom petroleum sludge in Oman. Journal of Hazardous Materials, 141, 557–564.

8. Allwar, A. 2012. Characteristics of pore structures and surface chemistry of activated carbons by physisorption, Ftir And Boehm methods. IOSR Journal of Applied Chemistry, 2, 9–15.

9. Azimi, S., Rocher, V., Muller, M., Moilleron, R., Thevenot, D.R. 2005. Sources, distribution and variability of hydrocarbons and metals in atmospheric deposition in an urban area (Paris, France). Science of the Total Environment, 337, 223–239.

10. Benzaoui, T., Selatnia, A. Djabali, D. 2018. Adsorption of copper (II) ions from aqueous solution using bottom ash of expired drugs incineration. Adsorption Science Technology, 36, 114–129.

11. Cai, L., Zhang, Y., Zhou, Y., Zhang, X., Ji, L., Song, W. et al. 2019a. Effective Adsorption of Diesel Oil by Crab-Shell-Derived Biochar Nanomaterials. Materials, 12, 236.

12. Cai, L., Zhang, Y., Zhou, Y., Zhang, X., Ji, L., Song, W. et al. 2019b. Effective adsorption of diesel oil by crab-shell-derived biochar nanomaterials. Materials, 12, 236.

13. Chikere, C.B., Okpokwasili, G.C., Chikere, B.O. 2011. Monitoring of microbial hydrocarbon remediation in the soil. 3 Biotech, 1, 117–138.

14. Diaz de Tuesta, J.L., Silva, A.M.T., Faria, J.L., Gomes, H.T. 2018. Removal of Sudan IV from a simulated biphasic oily wastewater by using lipophilic carbon adsorbents. Chemical Engineering Journal, 347, 963–971.

15. Djilani, C., Zaghdoudi, R., Modarressi, A., Rogalski, M., Djazi, F., Lallam, A. 2012. Elimination of organic micropollutants by adsorption on activated carbon prepared from agricultural waste. Chemical Engineering Journal, 189–190, 203–212.

16. Doczekalska, B., Bartkowiak, M., Łopatka, H., Zborowska, M. 2022. Activated carbon prepared from corn biomass by chemical activation with potassium hydroxide. BioResources, 17.

17. El Shahawy, A., Heikal, G. 2018. Organic pollutants removal from oily wastewater using clean technology economically, friendly biosorbent (Phragmites australis). Ecological Engineering, 122, 207–218.

18. Erto, A., Chianese, S., Lancia, A., Musmarra, D. 2017. On the mechanism of benzene and toluene adsorption in single-compound and binary systems: Energetic interactions and competitive effects. Desalination And Water Treatment, 86, 259–265.

19. Ewis, D., Mahmud, N., Benamor, A., Ba-Abbad, M.M., Nasser, M., El-Naas, M. 2022. Enhanced removal of diesel oil using new magnetic bentonite-based adsorbents combined with different carbon sources. Water, Air, Soil Pollution, 233, 195.

20. Farah, J., El-Gendy, N., Farahat, L. 2007. Biosorption of Astrazone Blue basic dye from an aqueous solution using dried biomass of Baker's yeast. Journal of Hazardous Materials, 148, 402–408.

21. Fernandez, M.E., Nunell, G.V., Bonelli, P.R., Cukierman, A.L. 2014. Activated carbon developed from orange peels: Batch and dynamic competitive adsorption of basic dyes. Industrial Crops and Products, 62, 437–445.

22. Foo, K., Hameed, B. 2011. Preparation of activated carbon from date stones by microwave induced chemical activation: application for methylene blue adsorption. Chemical Engineering Journal, 170, 338–341.

23. Gmach, O., Bertsch, A., Bilke-Krause, C., Kulozik, U. 2019. Impact of oil type and pH value on oil-in-water emulsions stabilized by egg yolk granules. Colloids and Surfaces A: Physicochemical and Engineering Aspects, 581, 123788.

24. Guo, Y., Tan, C., Sun, J., Li, W., Zhang, J. Zhao, C. 2020. Porous activated carbons derived from waste sugarcane bagasse for CO2 adsorption. Chemical Engineering Journal, 381, 122736.

25. Hazzaa, R. Hussein, M. 2015. Adsorption of cationic dye from aqueous solution onto activated carbon prepared from olive stones. Environmental Technology Innovation, 4, 36–51.

26. Húmpola, P., Odetti, H., Fertitta, A., Vicente, J. 2013. Thermodynamic analysis of adsorption models of phenol in liquid phase on different activated carbons. Journal of the Chilean Chemical Society, 58, 1541–1544.

27. Ingole, R.S., Lataye, D.H., Dhorabe, P.T. 2017. Adsorption of phenol onto banana peels activated carbon. KSCE Journal of Civil Engineering, 21, 100–110.

28. Jabbar, N.M., Salman, S.D., Rashid, I.M., Mahdi, Y.S. 2022. Removal of an anionic Eosin dye from aqueous solution using modified activated carbon prepared from date palm fronds. Chemical Data Collections, 42, 100965.

29. Jiang, J., Sun, K. 2017. Review on preparation technology of activated carbon and its application. Chemistry and Industry of Forest Products, 37, 1–13.

30. Shakir, K.I. 2010. Kinetic and isotherm modeling of adsorption of dyes onto Sawdust. Iraqi Journal of Chemical and Petroleum Engineering, 11, 15–27.

31. Khalid, M.W., Salman, S.D. 2019. Adsorption of heavy metals from aqueous solution onto sawdust activated carbon. Al-Khwarizmi Engineering Journal, 15, 60–69.

32. Khare, P., Baruah, B.P. 2010. Structural Parameters of Perhydrous Indian Coals. International Journal of Coal Preparation and Utilization, 30, 44–67.

33. Khatab E., Talib Salman, S.D. 2023. Removal of

malachite green from aqueous solution using ficus benjamina activated carbon-metal oxide synthesized by pyro carbonic acid microwave. Desalination and Water Treatment, 302, 105–209.

34. Labied, R., Benturki, O., Eddine Hamitouche, A.Y., Donnot, A. 2018. Adsorption of hexavalent chromium by activated carbon obtained from a waste lignocellulosic material (Ziziphus jujuba cores): kinetic, equilibrium, and thermodynamic study. Adsorption Science Technology, 36, 1066-1099.

35. Langmuir, I. 1917. The constitution and fundamental properties of solids and liquids. Journal of the Franklin Institute, 183, 102–105.

36. Li, W., Zhang, L.B., Peng, J.H., Li, N., Zhu, X.Y. 2008. Preparation of high surface area activated carbons from tobacco stems with K2CO3 activation using microwave radiation. Industrial Crops and Products, 27, 341–347.

37. Li, Z., Li, Y., Zhu, J. 2021. Straw-based activated carbon: optimization of the preparation procedure and performance of volatile organic compounds adsorption. Materials (Basel), 14.

38. Machín-Ramírez, C., Okoh, A., Morales, D., Mayolo-Deloisa, K., Quintero, R., Trejo-Hernández, M. 2008. Slurry-phase biodegradation of weathered oily sludge waste. Chemosphere, 70, 737–744.

39. Menya, E., Olupot, P., Storz, H., Lubwama, M., Kiros, Y. 2018. Production and performance of activated carbon from rice husks for removal of natural organic matter from water: a review. Chemical Engineering Research, 129, 271–296.

40. Mohammed, A.A., Al-Musawi, T.J., Kareem, S.L., Zarrabi, M., Al-Ma'abreh, A.M. 2020. Simultaneous adsorption of tetracycline, amoxicillin, and ciprofloxacin by pistachio shell powder coated with zinc oxide nanoparticles. Arabian Journal of Chemistry, 13, 4629–4643.

41. Nasrullah, A., Khan, H., Khan, A.S., Man, Z., Muhammad, N., Khan, M.I., El-Salam, N.M.A. 2015. Potential biosorbent derived from Calligonum polygonoides for removal of methylene blue dye from aqueous solution. Scientific World Journal, 2015, 562693.

42. Nowicki, P., Pietrzak, R., Wachowska, H. 2010. Sorption properties of active carbons obtained from walnut shells by chemical and physical activation. Catalysis Today, 150, 107–114.

43. Osman, A.I., Blewitt, J., Abu-Dahrieh, J.K., Farrell, C., Al-Muhtaseb, A.A.H., Harrison, J., Rooney W.D. 2019. Production and characterisation of activated carbon and carbon nanotubes from potato peel waste and their application in heavy metal removal. Environmental Science and Pollution Research, 26, 37228–37241.

44. Özdemir, M., Bolgaz, T., Saka, C. Şahin, Ö. 2011. Preparation and characterization of activated carbon from cotton stalks in a two-stage process. Journal of Analytical and Applied Pyrolysis, 92, 171–175.

45. Pan, X., Zhang, D. Quan, L. 2007. Interactive factors leading to dying-off Carex tato in Momoge wetland polluted by crude oil, Western Jilin, China. Chemosphere, 65, 1772–1777.

46. Puziy, A.M., Poddubnaya, O.I., Martínez-Alonso, A., Suárez-García, F. Tascón, J.M.D. 2002. Synthetic carbons activated with phosphoric acid: I. Surface chemistry and ion binding properties. Carbon, 40, 1493–1505.

47. Rasouli, Y., Abbasi, M. Hashemifard, S.A. 2017. Oily wastewater treatment by adsorption–membrane filtration hybrid process using powdered activated carbon, natural zeolite powder and low cost ceramic membranes. Water Science and Technology, 76, 895–908.

48. Saleem, J., Shahid, U.B., Hijab, M., Mackey, H. McKay, G. 2019. Production and applications of activated carbons as adsorbents from olive stones. Biomass Conversion and Biorefinery, 9, 775–802.

49. Salman, G.M.A.H.S.D. 2020. Adsorption of Para Nitro-phenol by Activated Carbon produced from Alhagi Sains Malaysiana 49, 57–67.

50. Salman, J.M., Njoku, V.O., Hameed, B.H. 2011. Bentazon and carbofuran adsorption onto date seed activated carbon: Kinetics and equilibrium. Chemical Engineering Journal, 173, 361–368.

51. Salman, S.D., Rasheed, I.M., Ismaeel, M.M. 2023. Removal of diclofenac from aqueous solution on apricot seeds activated carbon synthesized by pyro carbonic acid microwave. Chemical Data Collections, 43, 100982.

52. Salman, S.D., Rasheed, I.M., Mohammed, A.K. 2021. Adsorption of heavy metal ions using activated carbon derived from Eichhornia (water hyacinth). IOP Conference Series: Earth and Environmental Science, 779, 012074.

53. Salman, S.D. Rashid, I.M. Production and characterization of composite activated carbon from potato peel waste for cyanide removal from aqueous solution. Environmental Progress & Sustainable Energy, e14260.

54. Salman, S.D. Rashid, I.M. 2024. Production and characterization of composite activated carbon from potato peel waste for cyanide removal from aqueous solution. Environmental Progress & Sustainable Energy, 43, e14260.

55. Şentorun-Shalaby, Ç.D., Uçak-Astarlıoğˇlu, M.G., Artok, L. Sarıcı, Ç. 2006. Preparation and characterization of activated carbons by one-step steam pyrolysis/activation from apricot stones. Microporous and Mesoporous Materials., 88, 126–134.

56. Seyed-Hosseini, N. Fatemi, S. 2013. Experimental study and adsorption modeling of COD reduction by activated carbon for wastewater treatment of oil refinery. Iranian Journal Of Chemistry Chemical Engineering-International English Edition, 32(81).

57. Sokker, H.H., El-Sawy, N.M., Hassan, M.A., El-Anadouli, B.E. 2011. Adsorption of crude oil from aqueous solution by hydrogel of chitosan based polyacrylamide prepared by radiation induced graft polymerization. Journal of Hazardous Materials, 190, 359–365.

58. Suzuki, R.M., Andrade, A.D., Sousa, J.C., Rollemberg, M.C. 2007. Preparation and characterization of activated carbon from rice bran. Bioresource Technology, 98, 1985–1991.

59. Taşar, Ş., Kaya, F. Özer, A. 2014. Biosorption of lead(II) ions from aqueous solution by peanut shells: Equilibrium, thermodynamic and kinetic studies. Journal of Environmental Chemical Engineering, 2, 1018–1026.

60. Tseng, R.L. Tseng, S.K. 2005. Pore structure and adsorption performance of the KOH-activated carbons prepared from corncob. Journal of Colloid and Interface Science, 287, 428–437.

61. Vaghetti, J.C.P., Lima, E.C., Royer, B., Cardoso, N.F., Martins, B. Calvete, T. 2009. Pecan nutshell as biosorbent to remove toxic metals from aqueous solution. Separation Science and Technology, 44, 615–644.

62. Van der Bruggen, B. 2015. Freundlich Isotherm. In: encyclopedia of membranes (eds. Drioli, E Giorno, L). Springer Berlin Heidelberg Berlin, Heidelberg. 1–2.

63. Wei, D., Zhang, H., Cai, L., Guo, J., Wang, Y., Ji, L., Song W. 2018. Calcined mussel shell powder (cmsp) via modification with surfactants: application for antistatic oil-removal. Materials, 11.

64. Yagmur, E., Ozmak, M., Aktas, Z. 2008. A novel method for production of activated carbon from waste tea by chemical activation with microwave energy. Fuel, 87, 3278–3285.

65. Yang, D., Jiang, L., Yang, S., Wei, S. 2017. Experimental study on preparation of straw activated carbon by microwave heating. Procedia Engineering, 205, 3538–3544.

66. Yang, K., Zhu, L., Yang, J., Lin, D. 2018. Adsorption and correlations of selected aromatic compounds on a KOH-activated carbon with large surface area. Science of the Total Environment, 618, 1677–1684.

67. Yeddou, A.R., Nadjemi, B., Halet, F., Ould-Dris, A., Capart, R. 2010. Removal of cyanide in aqueous solution by oxidation with hydrogen peroxide in presence of activated carbon prepared from olive stones. Minerals Engineering, 23, 32–39.

68. Zhang, B., Dong, Z., Sun, D., Wu, T.L.Y. 2017. Enhanced adsorption capacity of dyes by surfactant-modified layered double hydroxides from aqueous solution. Journal of Industrial and Engineering Chemistry, 49, 208–218.